



National Defence  
Défense nationale

UNCLASSIFIED

DTIC FILE COPY

UNLIMITED  
DISTRIBUTION

**DRES**

## SUFFIELD MEMORANDUM

NO. 1124

SENSITIVITY OF SFF COMPUTER SIMULATIONS  
TO VARIATIONS IN THE JWL EQUATION OF STATE (U)

DTIC  
ELECTE  
FEB 02 1990  
S D D

by

K.R. Torrance

**DISTRIBUTION STATEMENT A**

Approved for public release.  
Distribution Unlimited

PCN No. 27C20

January 1985



DEFENCE RESEARCH ESTABLISHMENT SUFFIELD, RALSTON, ALBERTA

**WARNING**

The use of this information is permitted subject to  
recognition of proprietary and patent rights.

Canada

9 0 02 02 0 54

UNCLASSIFIED

DEFENCE RESEARCH ESTABLISHMENT SUFFIELD  
RALSTON ALBERTA

SUFFIELD MEMORANDUM NO. 1124

SENSITIVITY OF SFF COMPUTER SIMULATIONS  
TO VARIATIONS IN THE JWEL EQUATION OF STATE (U)

by

K.R. Torrance

PCN No. 27C20

Accession For	
NTIS CR4&I	<input checked="checked" type="checkbox"/>
DTIC TAB	<input type="checkbox"/>
Unannounced	<input type="checkbox"/>
Justification	
By	
Distribution/	
Availability Codes	
Dist	Avail and/or Special
A-1	

**WARNING**  
The use of this information is permitted subject to recognition  
of proprietary and patent rights.



UNCLASSIFIED

UNCLASSIFIED

DEFENCE RESEARCH ESTABLISHMENT SUFFIELD  
RALSTON ALBERTA

SUFFIELD MEMORANDUM NO. 1124

**SENSITIVITY OF SFF COMPUTER SIMULATIONS  
TO VARIATIONS IN THE JWL EQUATION OF STATE (U)**

by

K.R. Torrance

**ABSTRACT**

*8/* The sensitivity of predictions of self-forging fragment shape and kinetic energy to variations in the Jones-Wilkins-Lee (JWL) equation of state for the detonation products is studied parametrically using the EPIC-2 finite element computer code. JWL parameters are varied for two warhead designs: the EXROD (EXplosive Remote Opening Device) and the REDM (REsearch and Development Munition). The resulting percentage changes in shape factor and kinetic energy are presented in tabular and graphical form, and the most influential JWL parameters are identified. //

(ii)

UNCLASSIFIED

UNCLASSIFIED

### **ACKNOWLEDGEMENTS**

The author is indebted to Mr. Michael G. Kramer who, while a Summer Research Assistant at DRES, performed half of the computer simulations necessary and contributed to preliminary evaluation of the data, and to Dr. Allan W. Gibb for providing supervision throughout.

(iii)

UNCLASSIFIED

UNCLASSIFIED

## TABLE OF CONTENTS

	Page No.
ABSTRACT .....	li
ACKNOWLEDGEMENTS .....	iii
TABLE OF CONTENTS .....	iv
LIST OF TABLES .....	v
LIST OF FIGURES .....	vi
1.0 INTRODUCTION .....	1
1.1 Background .....	1
1.2 Description of EPIC-2 .....	2
1.3 Self-Forging Fragment Devices .....	3
1.4 JWL Equation of State .....	3
2.0 PARAMETER VARIATIONS .....	4
3.0 PRESENTATION OF RESULTS .....	6
3.1 Fragment Shape .....	6
3.2 Fragment Kinetic Energy .....	7
4.0 DISCUSSION OF RESULTS .....	7
4.1 General .....	7
4.2 Fragment Shape .....	8
4.3 Fragment Dynamics .....	9
5.0 CONCLUSIONS AND RECOMMENDATIONS .....	9
6.0 REFERENCES .....	11

APPENDIX — EXROD AND REDM FINAL FRAGMENT SHAPES

(iv)

UNCLASSIFIED

UNCLASSIFIED

## LIST OF TABLES

Table 1	Range of Known JWL Coefficients for Most High Explosives
Table 2	Shape Factor Data for EXROD and REDM Fragments
Table 3	Drag Coefficients for EXROD Fragments
Table 4	Velocity Data for EXROD and REDM Fragments

UNCLASSIFIED

UNCLASSIFIED

## LIST OF FIGURES

- Figure 1 Self-Forging Fragment Device
- Figure 2 EPIC-2 Representation of the REDM Warhead
- Figure 3 EPIC-2 Representation of the EXROD Warhead
- Figure 4 REDM Final Fragment Shapes for 2 Representative Parameter Variations
- Figure 5 EXROD Final Fragment Shapes for 2 Representative Parameter Variations
- Figure 6 Definition of the Shape Factor  $l/d$  for the EXROD and REDM Fragments
- Figure 7 Percent Changes in EXROD and REDM Shape Factor ( $l/d$ ) for Each Parameter Variation
- Figure 8 Forebody Drag of a Group of Spheroidal Heads as a Function of Forebody Length Ratio at  $M = 1.6$
- Figure 9 Theoretical and Experimental Drag Coefficients of Various Conical Heads at Transonic and Supersonic Mach Numbers
- Figure 10 Percent Changes in EXROD  $C_D$  for Each Parameter Variation
- Figure 11 Percent Changes in EXROD and REDM Kinetic Energies for Each Parameter Variation

UNCLASSIFIED

①  
UNCLASSIFIED

DEFENCE RESEARCH ESTABLISHMENT SUFFIELD  
RALSTON ALBERTA

SUFFIELD MEMORANDUM NO. 1124

**SENSITIVITY OF SFF COMPUTER SIMULATIONS  
TO VARIATIONS IN THE JWEL EQUATION OF STATE (U)**

by

K.R. Torrance

**1.0 INTRODUCTION**

**1.1 Background**

During the course of a confrontation, Canadian Forces military engineers employ explosives and shaped charges to destroy bridges and other structures in a counter-mobility role. Currently, these charges must be physically attached to the structure being demolished, often a difficult and time-consuming task. As an alternative, the self-forging fragment (SFF) type of projectile, used for example in off-route anti-tank mines, is under study at DRES to see if it could provide military engineers with a long-standoff rapid demolition capability. The development of a long-standoff SFF wall-breaching device is also being pursued.

UNCLASSIFIED



In studying the application of self-forging fragment technology to the demolition role, a reduction in the size and cost of an experimental field program is afforded by the use of finite element computer codes which can predict both fragment formation and target impact. An important factor in obtaining a reasonable prediction of fragment formation is the use of an accurate pressure-volume relationship for the explosive's detonation products. This relationship is given by the Jones-Wilkins-Lee (JWL) equation of state. For many explosives, the coefficients of the JWL equation have been tabulated in the literature. However, for some explosives of interest for potential use in SFF devices, the JWL coefficients have not been published. In such cases, estimates must be made based on explosives of similar properties. It is of considerable interest to know what effect inaccurate estimates would have on predicted fragment characteristics.

Such considerations provided the motivation for the study reported herein. The sensitivity of predictions of the EPIC-2 computer code (1) to changes in the JWL equation of state for two SFF warhead designs are investigated: the EXROD (Explosive Remote Opening Device) and the REDM (Research and Development Munition).

## **1.2 Description of EPIC-2**

The EPIC-2 (Elastic-Plastic-Impact Computations in 2 Dimensions) code is based on a Lagrangian finite element formulation where the equations of motion are integrated directly, rather than through the traditional stiffness matrix approach. The formulation uses a triangular element, which is well-suited to representing the severe distortions which often occur during fragment formation. Although the code is arranged to provide solutions for projectile-target impact and explosively-formed projectiles, the basic formulation is valid for a wide range of problems involving dynamic responses of continuous media. The code is applicable to axisymmetric and plane strain problems. It also has the capability to handle the effect of spin for the axisymmetric case. The EPIC-2 code includes nonlinear material strength and compressibility effects to account for elastic-plastic flow and wave propagation. It has an elastic-plastic material model in which strain hardening, strain rate, and thermal softening effects can be included. It has a mesh generator to construct meshes for various simple shapes. It has the capability to include multiple sliding surfaces. The post-processor provides plots of initial and deformed geometry as well as stress, strain, pressure and velocity fields. It also has the capability to produce time-dependent plots of various system parameters.

### 1.3 Self-forging Fragment Devices

Briefly, a typical SFF device, as depicted in Figure 1 (2), consists of a high explosive charge, metal liner, body and an initiation system. When the explosive is initiated, a detonation wave traverses the high explosive and contacts the metal liner, forming it into a single non-molten slug or fragment travelling at a velocity of typically 1 -- 3 km/sec. Useful ranges for these warheads can vary from 10 m to 300 m, depending upon the application.

The two SFF devices which were the parent designs of this parametric study will now be discussed in more detail.

**REDM** — Developed specifically for the experimental investigation of SFF formation and target impact, this axisymmetric warhead design utilizes a 1.7 kg Octol 75/25 explosive filling to drive a 143 mm diameter OFHC copper liner. The finite element representation of this design is illustrated in Figure 2.

**EXROD** — This second axisymmetric SFF, whose finite element model is shown in Figure 3, was developed primarily for explosive ordnance disposal applications; hence its smaller size compared to the REDM. In this design, a 500 g Octol 70/30 charge propels a 73 mm diameter SAE 1020 steel liner.

### 1.4 JWL Equation of State

An explosive equation of state is an essential part of any SFF computer model. Its purpose is to predict the pressure of the detonation products as the detonation wave propagates through the solid explosive. The liner is then in turn deformed by this pressure into a slug or fragment travelling at high velocity. The Jones-Wilkins-Lee (JWL) equation of state is chosen because it can accurately describe the behaviour of the detonation products over the extremely high pressure regime encountered. The JWL equation of state (3) is:

$$P = A(1 - \omega/R_1 V)e^{-R_1 V} + B(1 - \omega/R_2 V)e^{-R_2 V} + \omega E/V \quad [1]$$

where  $P$  = pressure (GPa)

$V$  = (volume of detonation products)/(volume of undetonated explosive)  
= relative volume

$E$  = internal energy per unit volume (GPa)

$A, B$  = linear coefficients (GPa)

$\omega$  = dimensionless linear coefficient

$R_1, R_2$  = dimensionless non-linear coefficients

The five JWL coefficients published for 78/22 Octol (4) are:

$$A = 748.6 \text{ GPa}$$

$$B = 13.38 \text{ GPa}$$

$$R_1 = 4.50$$

$$R_2 = 1.20$$

$$\omega = 0.38$$

with  $E = 9.60 \text{ GPa}.$

EPIC-2 simulations of the REDM and EXROD geometries performed with the above values for the five JWL coefficients will henceforth be referred to as the parent cases. In this study, these five coefficients will be varied in the EPIC code and their respective effects on the REDM and EXROD fragment shapes and dynamics compared to the parent cases.

## 2.0 PARAMETER VARIATIONS

Before selecting the changes in the five JWL parameters from the parent case, it is first necessary to recognize limits on their range of possible values. To begin with, since  $P$  is positive,  $A$ ,  $B$ ,  $R_1$ ,  $R_2$  and  $\omega$  must all be non-negative. Secondly,  $R_1$  and  $R_2$  must always be greater than or equal to  $\omega/V$  to ensure that  $P$  is positive. The limiting case occurs at the Chapman-Jouguet point where  $V$  is at a minimum. This volume, the Chapman-Jouguet relative volume, can be calculated from simple 1-dimensional detonation theory (3) as shown below:

$$V_{CJ} = 1 - P_{CJ}/\rho_0 D^2$$

where  $V_{CJ}$  = Chapman-Jouget relative volume

$P_{CJ}$  = Chapman-Jouget pressure

$\rho_0$  = initial density

$D$  = detonation velocity

For 78/22 Octol, these constants have the following values (4):

$$P_{CJ} = 34.2 \text{ GPa}$$

$$\rho_0 = 1.821 \text{ g/cm}^3$$

$$D = 8.48 \text{ mm}/\mu\text{s}$$

yielding a Chapman-Jouguet relative volume of 0.74. Hence, for  $\omega = 0.38$ , both  $R_1$  and  $R_2$  must always be greater than or equal to 0.51.

It was decided at the outset of the project that a parametric study which took into account all possible combinations of variations in A, B,  $R_1$ ,  $R_2$  and  $\omega$ , while desirable in principle, would be impractical in practice due to the excessively large number of computer runs required. It was decided to limit the study to single parameter variations, i.e., to cases in which one parameter was varied while the four remaining ones were maintained at their parent values.

It was necessary to establish a range of values for each parameter variation. A guide as to a suitable magnitude for each parameter change is the range of values of that parameter for all high explosives for which JWL data are available. Table 1 lists the maximum and minimum measured values for each JWL coefficient, regardless of explosive composition, expressed as a percent deviation from the respective coefficient for Octol 78/22. It was also considered advantageous to standardize the relative magnitude of each parameter change, so as to simplify comparison of the effect of varying different parameters. Lastly, preliminary tests indicated that substantial changes in the linear parameters (greater than 50%) were required to detect significant differences in fragment shape and dynamics. After consideration of these factors, a standard variation for each parameter of  $\pm 100\%$  about the parent values was chosen, except for  $R_1$  and  $R_2$  which cannot be reduced by 100% for the previously-cited reason. Instead,  $R_1$  and  $R_2$  were each reduced by 20%. This percentage reduction produces values which are still within the known minimum range of values for these two coefficients (see Table 1) and also satisfies the constraint  $R_1, R_2 \geq 0.51$ .

The final strategy for parameter variations became:

$$\begin{aligned} A &\pm 100\% \\ B &\pm 100\% \\ R_1 &+ 100\%, - 20\% \\ R_2 &+ 100\%, - 20\% \\ \omega &\pm 100\% \end{aligned}$$

Each coefficient was altered one at a time, making for a total of ten EPIC code calculations for each of the two SFF designs. In addition, one calculation was carried out using the parent parameters for each of the REDM and EXROD designs.

### 3.0 PRESENTATION OF RESULTS

#### 3.1 Fragment Shape

Fully-formed fragment shapes predicted by EPIC-2 for both the REDM and EXROD geometries are illustrated in Figures 4 and 5 respectively. Two representative parameter variations (REDM:  $A + 100\%$ ,  $A - 100\%$ ; EXROD:  $R_1 + 100\%$ ,  $R_2 - 20\%$ ) are shown for comparison with each parent parameter case. As noted in these figures and verified by flash x-radiographs of the parent cases, the material comprising the liner edges fails and breaks away from the main body during the initial stages of fragment formation and hence can be ignored for the purposes of comparison. A complete catalogue of REDM and EXROD fragment shapes for each parameter change is contained in the appendix.

A quantitative measure of fragment shape change was introduced in the form of a dimensionless geometric shape factor, defined in Figure 6. If one ignores the liner edges (since they break off, as explained previously) and the uneven convex nose (which is an artifact of the computation process related solely to mesh size), the EXROD fragment's exterior profile can be approximated as a bullet-nosed projectile of diameter  $d$  and nose length  $l$  with a negligible cylindrical afterbody. Again ignoring the liner edges, the REDM fragment's exterior profile can be approximated as a right circular cone of base diameter  $d$  and height  $l$ . The dimensionless shape factor for both geometries is then simply the ratio  $l/d$ .

The percentage changes in shape factor between each parameter variation and the parent case are given in bar chart form in Figure 7 for both the REDM and EXROD geometries. The shape factors themselves are tabulated in Table 2.

An alternative measure of fragment shape change employs the change in drag coefficient. This approach, however, has more restricted applications than the shape factor as drag data at hypersonic speeds are available for only a limited range of geometries. In the case of the highly non-aerodynamic REDM fragment, such drag data are unavailable. The EXROD fragment, on the other hand, lends itself well to this approach. Figure 8 presents drag coefficients for bullet-nosed bodies similar in shape to the EXROD fragment. As drag data are given at  $M = 1.6$ , whereas the EXROD fragment travels at an approximate speed of  $M = 8$ , the absolute magnitudes of  $C_D$  will be overpredicted since  $C_D$  decreases with increasing supersonic Mach number (see

Figure 9). However, it is the changes in drag coefficient relative to that of the parent case that is of primary interest. Over the narrow range of  $x/d$  values for the EXROD fragments (.26 – 1.28), the drag coefficient curve at  $M = 8$  is assumed to be similar in form to that in Figure 8. In fact, in this application, the curve can be utilized as if it were valid for bodies at  $M = 8$  since the resulting overpredictions in drag coefficient will largely cancel one another when computing the percentage changes in  $C_d$  relative to the parent case drag coefficient. These percentage changes are presented in Figure 10 while the values of the drag coefficients are tabulated in Table 3.

### 3.2 Fragment Kinetic Energy

Most penetration theories correlate projectile kinetic energy, rather than projectile velocity, with target penetration. Therefore, fragment kinetic energy was chosen to characterize the effects of the parameter changes on fragment dynamics. Since the EPIC code does not account for drag forces on the fragment during its flight, the kinetic energies calculated are for a fragment just after it is fully formed, rather than just before striking a target some distance away. Figure 11 presents the percentage deviations in kinetic energy from the parent case of both the REDM and EXROD designs. Table 4 contains the raw velocity data from which the changes in kinetic energy were calculated.

## 4.0 DISCUSSION OF RESULTS

### 4.1 General

Changing the JWL parameters obviously alters the pressure predicted by this equation of state. By inspection of the JWL equation of state (equation 1), a change in any of the linear JWL coefficients,  $A$ ,  $B$  and  $\omega$ , produces a change in pressure of the same sign. Of the terms containing the non-linear coefficients,  $R_1$  and  $R_2$ , the negative exponentials dominate and hence a change in either of these two parameters produces a pressure change of opposite sign. Momentum is transferred from the detonation products to the liner in both the radial and axial directions. In the radial direction, an increase in the detonation products' pressure primarily causes the liner elements to converge more towards the axis. Axially, an increase in pressure primarily raises the forward velocity of the fragment. A decrease in the pressure predicted by the JWL equation of state produces opposite effects. The radial and axial effects of the parameter changes will be dealt with in the following two sections.

## 4.2 Fragment Shape

The main radial effect of variations in the five JWL parameters is on fragment shape. More specifically, the changes in detonation product pressure alter the radial movement of liner material towards the axis of symmetry. This movement of liner material will henceforth be referred to as radial convergence.

The effect of the linear parameter,  $A$ , on radial convergence is shown in Figure 4 using the REDM fragment as an example. An increase in the pressure of the detonation products caused by raising  $A$  by 100% resulted in a more slender final slug displaying much more radial convergence than the parent parameter case. Conversely, a decrease of the same amount in the  $A$  parameter yielded a squatter fragment with less radial convergence. Results of variations in the two remaining linear parameters,  $B$  and  $\omega$ , follow similar patterns.

The effect of the non-linear parameter,  $R_1$ , is shown in Figure 5 using the EXROD as an example this time. As  $R_1$  is the coefficient of a negative exponential term in the equation of state, a reduction in  $R_1$  of 20% raises the detonation products' pressure and produces a fragment exhibiting more radial convergence while an increase of 100% has the reverse effect. The other non-linear parameter,  $R_2$ , behaves similarly.

The quantified effects of JWL parameter changes on fragment shape, expressed as changes in the shape factor  $l/d$ , can be observed in the bar chart of Figure 7. Now the relative effect of each parameter on fragment shape emerges. As the first term in the JWL equation of state for Octol accounts for over 70% of the peak pressure generated at the CJ point (since  $A$  is much larger than  $B$  and  $E$ ), it is not unexpected that changes in the JWL coefficients in this term ( $A$  and  $R_1$ ) produce the greatest positive and negative variations in shape factor. The remaining coefficients,  $B$ ,  $\omega$  and  $R_2$ , attached to the second and third terms in the JWL equation of state, affect  $l/d$  to a lesser, though still significant, degree.

Notice the sign of the parameter change and the sign of the change in  $l/d$ . Positive changes (i.e., increases) in the three linear parameters,  $A$ ,  $B$  and  $\omega$ , cause positive changes in  $l/d$  since the resulting pressure increase drives the liner elements closer to the axis, raising the  $l/d$  ratio. Conversely, negative changes in the linear coefficients cause negative changes in  $l/d$ . Positive changes in the two non-linear parameters,  $R_1$  and  $R_2$ , cause negative changes (i.e., reductions) in  $l/d$  since they result in lowered pressures and hence less radial convergence of the liner. Conversely, negative changes in  $R_1$  and  $R_2$  will cause positive changes in  $l/d$ .

Due to the inverse relationship between  $C_D$  and  $l/d$  (see Figure 8), the alternate measure of fragment shape change, the drag coefficient, responds in a manner directly opposite to the shape factor  $l/d$ . That is, variations in the linear parameters result in changes of opposite sign in  $C_D$  while variations in the non-linear parameters produce changes of the same sign in  $C_D$ . Again, A and  $R_1$  are the most influential parameters, producing the greatest variations in  $C_D$ .

### 4.3 Fragment Dynamics

The main axial effect of JWL parameter changes is to alter the final kinetic energy of the fragment. The bar chart of Figure 11 details the influence of each parameter on the kinetic energies of both designs studied in this report. Changes in the linear parameters produce pressure changes of the same sign and hence kinetic energy changes of the same sign through the transfer of momentum from the detonation gases to the liner. Changes in the non-linear parameters produce pressure changes of the opposite sign and hence kinetic energy changes of the opposite sign. Also note that, here too, A and  $R_1$  are responsible for the greatest deviation.

It is noteworthy that the kinetic energy variations in Figure 11 for the REDM and EXROD designs are almost interchangeable. Since the REDM and EXROD form fragments of different shape, this result suggests that the effect of JWL parameter changes on fragment kinetic energy may be largely geometry-independent.

## 5.0 CONCLUSION AND RECOMMENDATIONS

For the parameter variations considered in this report, the greatest positive and negative effects in fragment shape and fragment dynamics for the two munitions under study are summarized below:

	EXROD	REDM
% change $l/d$	+ 100	+ 78
	- 59	- 41
% change K.E.	+ 41	+ 58
	- 30	- 30



All of the above changes in fragment characteristics were due to variations in the two most influential JWL parameters, A and  $R_1$ . Since the size of the parameter variations utilized in this study are generally much larger than those that would normally be encountered when applying the EPIC-2 code, the percentage changes in shape factor and kinetic energy represent an upper bound of what would occur in practice.

With respect to the parameter variations, this study has treated the JWL equation of state as an empirical relation in which the parameters can be varied independently. The constraints that simple one-dimensional detonation theory place on the equation of state have been ignored. These constraints would, in fact, establish a dependency among the parameter variations and limit their magnitudes of change. The method given in Reference 6 for obtaining JWL coefficients from cylinder test data may be used to establish this dependency. It is recommended that a future parametric study be carried out with variations thus constrained.

## 6.0 REFERENCES

1. "EPIC-2, A Computer Program for Elastic-Plastic Impact Computations in 2 Dimensions Plus Spin", Honeywell Inc., Defence Systems Division, Contract Report ARBRL-CR-00373, prepared for U.S. Army ARRADCOM, Ballistic Research Laboratory, June 1978. UNCLASSIFIED.
2. Hermann, J. W., Randers-Pehrson, G., and Berus, E. R., "Experimental and Analytical Investigation of Self-Forging Fragments for the Defeat of Armor at Extremely Long Standoff". Third International Symposium on Ballistics, Karlsruhe, W. Germany, 1977.
3. Fickett, W., and Davis, W. C., **Detonation**, University of California Press, 1979.
4. Dobratz, B. M., "LLNL Explosives Handbook. Properties of Chemical Explosives and Explosive Simulants", UCRL-52997, Lawrence Livermore National Laboratory, March 1981. UNCLASSIFIED.
5. Hoerner, S. F., **Fluid Dynamic Drag**, published by the author, 1958.
6. Bailey, W. A., Belcher, R. A., Chilvers, D. K., and Eden, G., "Explosive Equation of State Determination by the AWRE Method", Seventh Detonation Symposium, Annapolis, Md., U.S.A., 1981.

UNCLASSIFIED

**TABLE 1**

Range of known JWL coefficients for most high explosives expressed as a percent deviation from the respective coefficient for Octol 78/22.

JWL COEFFICIENT	% DEVIATION	
	MAX	MIN
A	+ 13	- 78
B	+ 74	- 76
R <sub>1</sub>	+ 56	- 14
R <sub>2</sub>	+ 67	- 21
$\omega$	+ 21	- 47

UNCLASSIFIED

UNCLASSIFIED

TABLE 2  
SHAPE FACTOR DATA FOR EXROD AND REDM FRAGMENTS

PARAMETER CHANGE	EXROD $l/d$	REDM $l/d$
parent case	0.64	5.63
A + 100%	1.28	9.55
A - 100%	0.26	3.32
B + 100%	0.93	6.78
B - 100%	0.35	4.81
$\omega$ + 100%	0.73	6.47
$\omega$ - 100%	0.46	3.50
R <sub>1</sub> + 100%	0.32	3.32
R <sub>1</sub> - 20%	1.26	10.00
R <sub>2</sub> + 100%	0.39	4.88
R <sub>2</sub> - 20%	0.71	5.67

UNCLASSIFIED

UNCLASSIFIED

**TABLE 3**  
**DRAG COEFFICIENTS FOR EXROD FRAGMENTS**

PARAMETER CHANGE	$x/d$	$C_D$
parent case	0.64	.585
A + 100%	1.28	.338
A - 100%	0.26	.854
B + 100%	0.93	.456
B - 100%	0.35	.769
$\omega$ + 100%	0.73	.538
$\omega$ - 100%	0.46	.692
$R_1$ + 100%	0.32	.800
$R_1$ - 20%	1.26	.346
$R_2$ + 100%	0.39	.738
$R_2$ - 20%	0.71	.546

UNCLASSIFIED

UNCLASSIFIED

TABLE 4  
VELOCITY DATA FOR EXROD AND REDM FRAGMENTS

PARAMETER CHANGE	EXROD VELOCITY (km/s)	REDM VELOCITY (km/s)
<del>parent case</del> parent case	<del>2.637</del> 2.637	<del>2.534</del> 2.534
A + 100%	3.059	2.948
A - 100%	2.276	2.118
B + 100%	2.951	2.858
B - 100%	2.281	2.178
$\omega$ + 100%	2.780	2.685
$\omega$ - 100%	2.327	2.240
R <sub>1</sub> + 100%	2.202	2.123
R <sub>1</sub> - 20%	3.129	3.187
R <sub>2</sub> + 100%	2.373	2.263
R <sub>2</sub> - 20%	2.763	2.649

UNCLASSIFIED

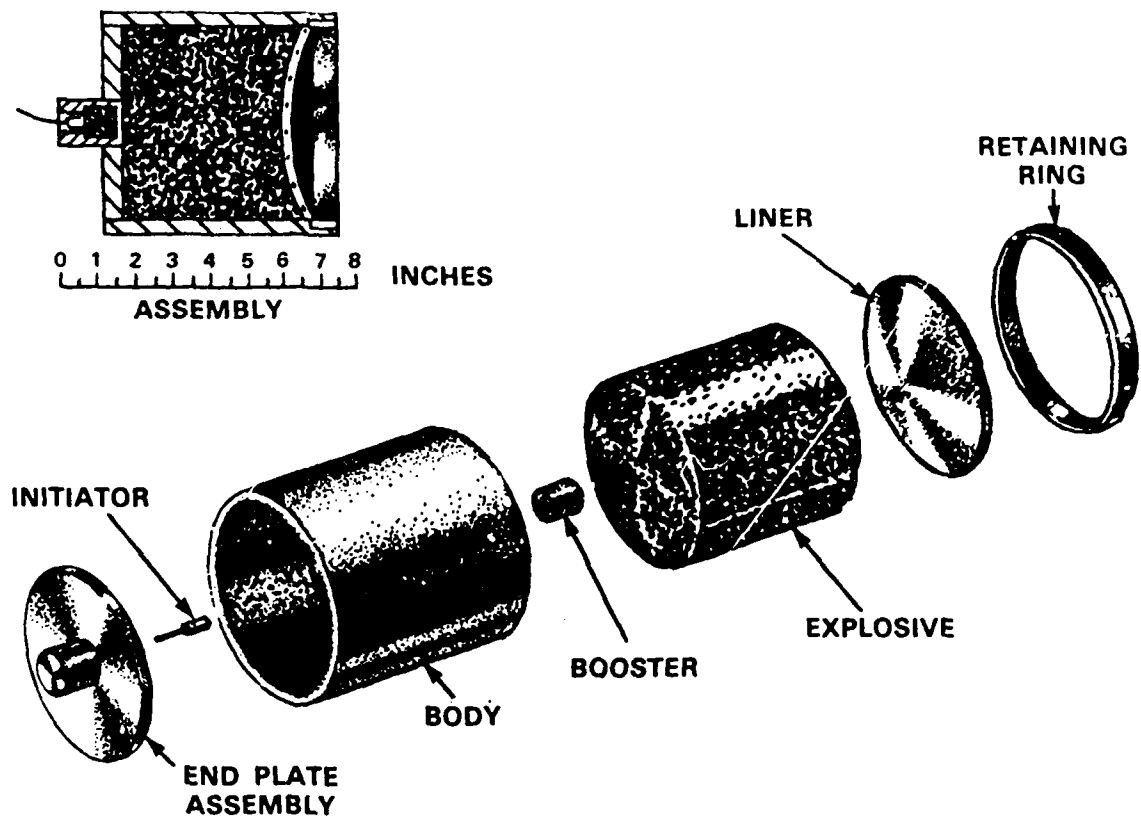


Figure 1

SELF-FORGING FRAGMENT DEVICE (REFERENCE 2)

UNCLASSIFIED

SM 1124

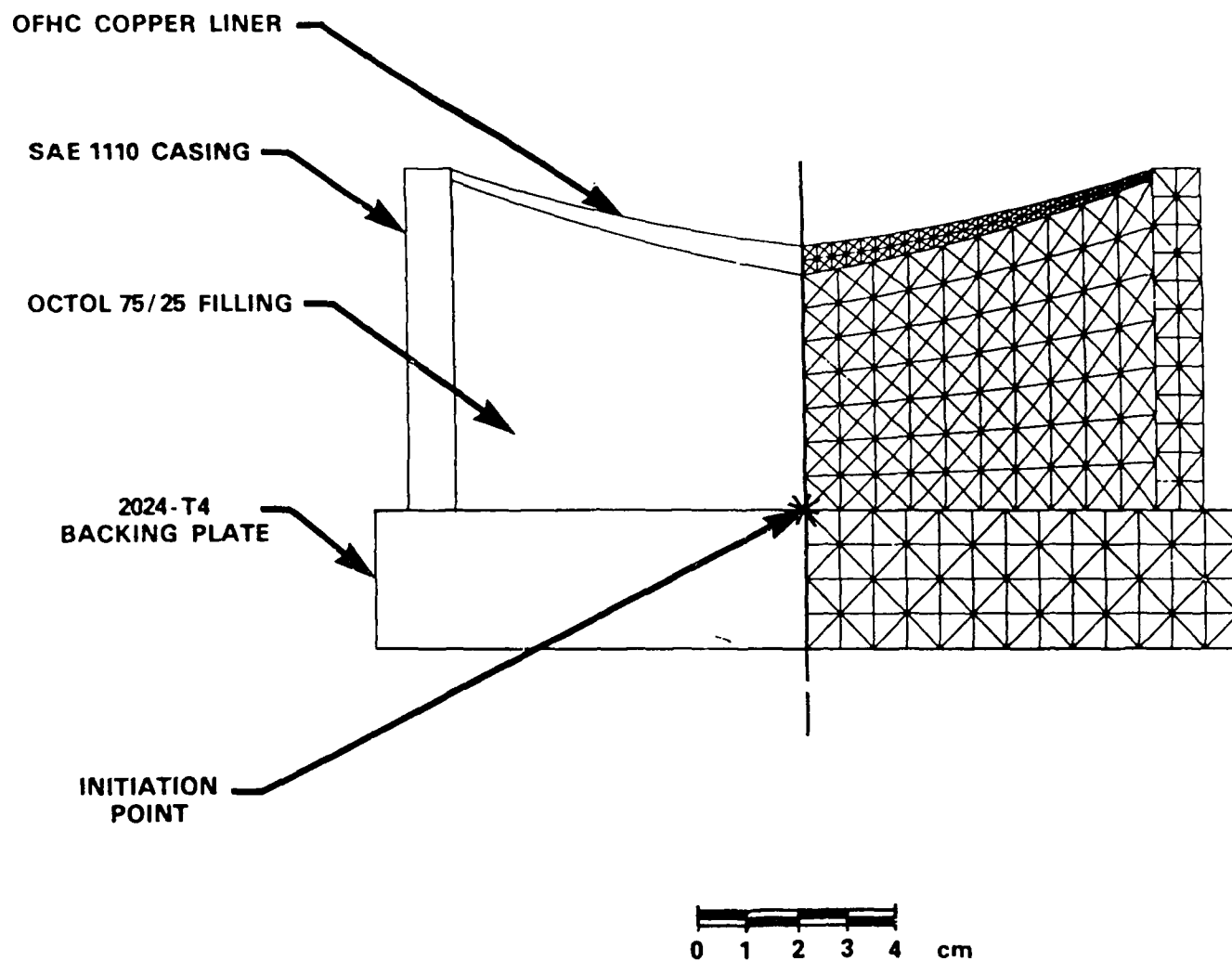


Figure 2

EPIC-2 REPRESENTATION OF THE REDM WARHEAD

UNCLASSIFIED



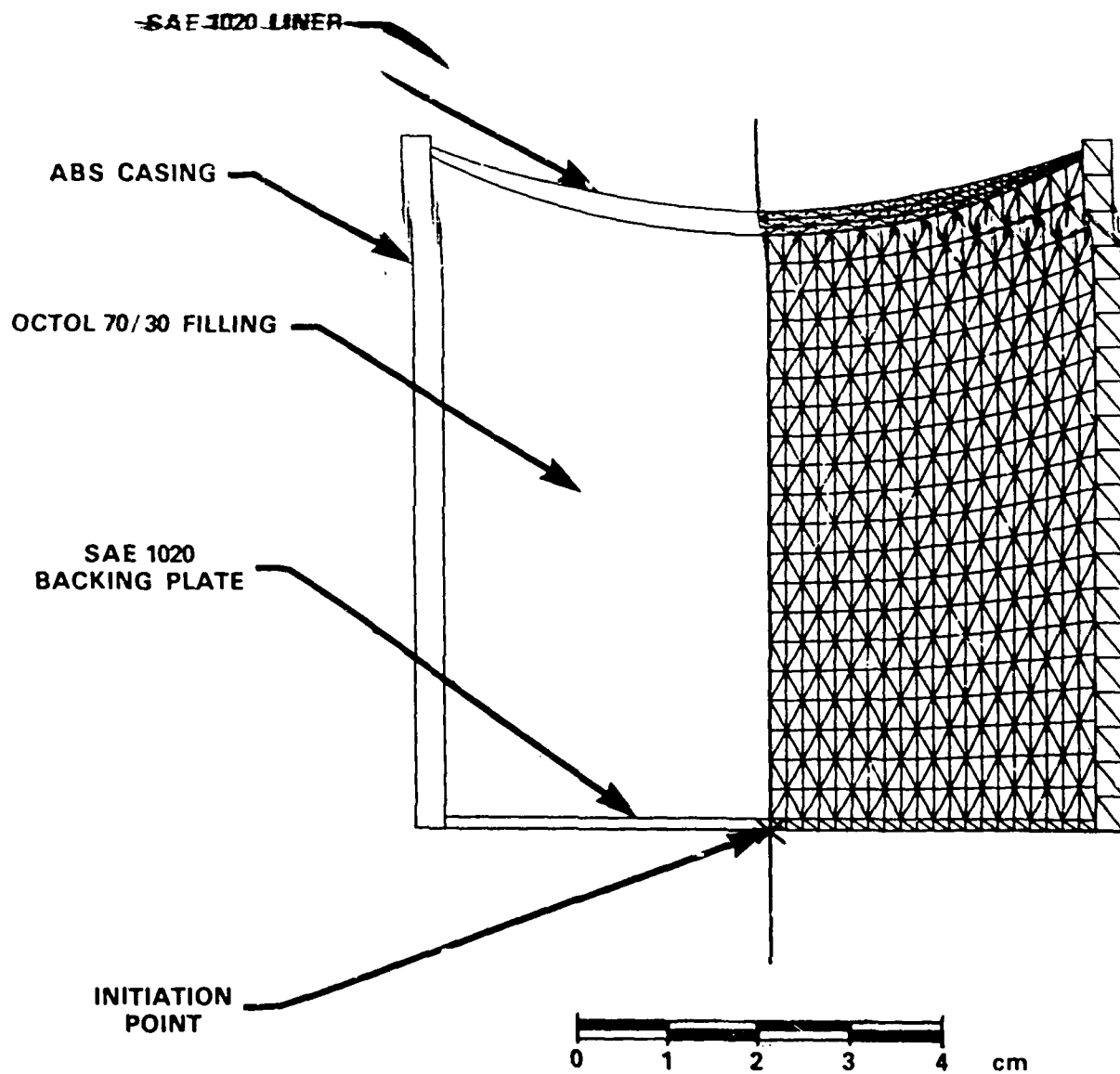


Figure 3

EPIC-2 REPRESENTATION OF THE EXROD WARHEAD

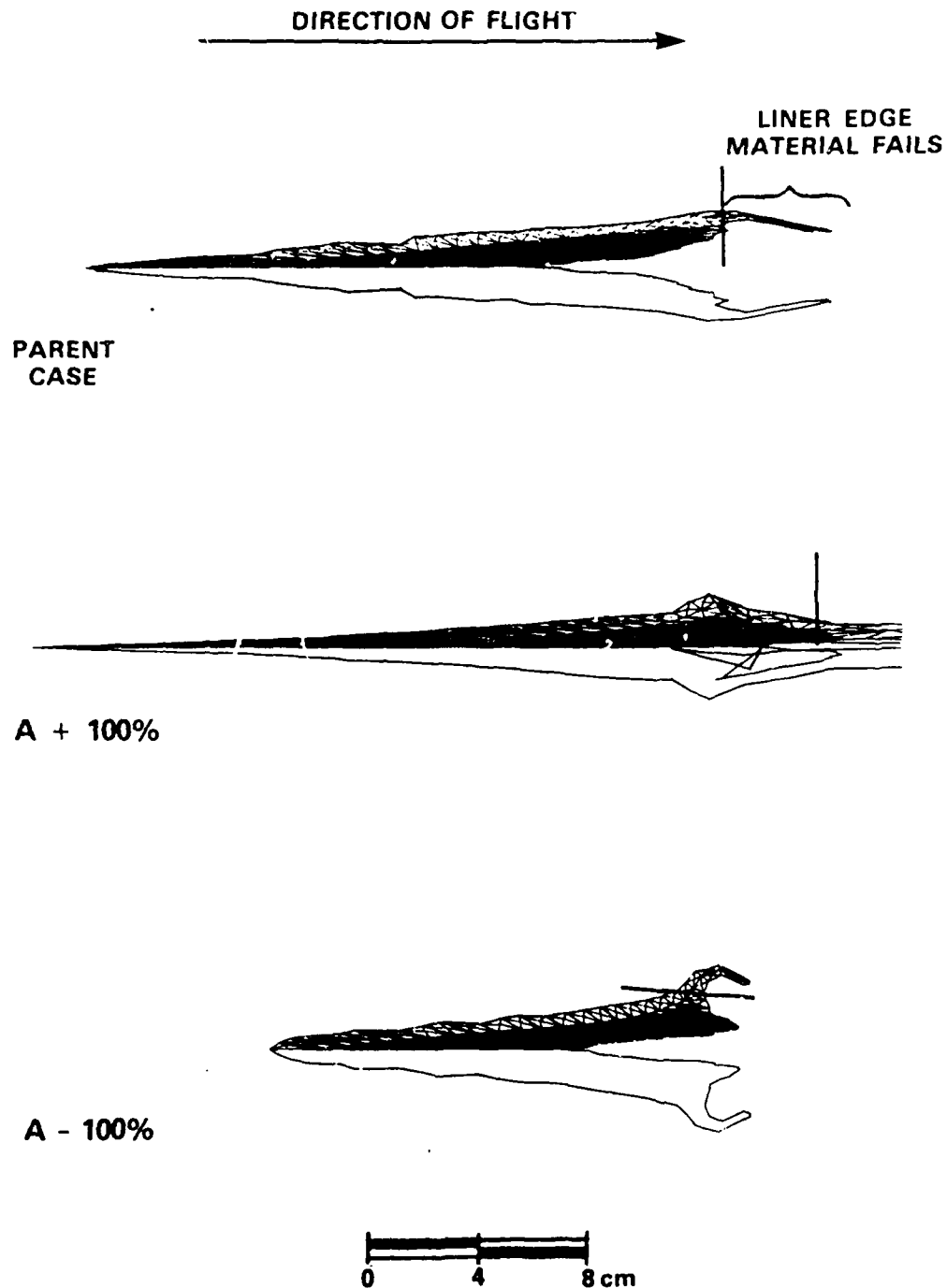


Figure 4

REDM FINAL FRAGMENT SHAPES FOR 2 REPRESENTATIVE  
PARAMETER VARIATIONS

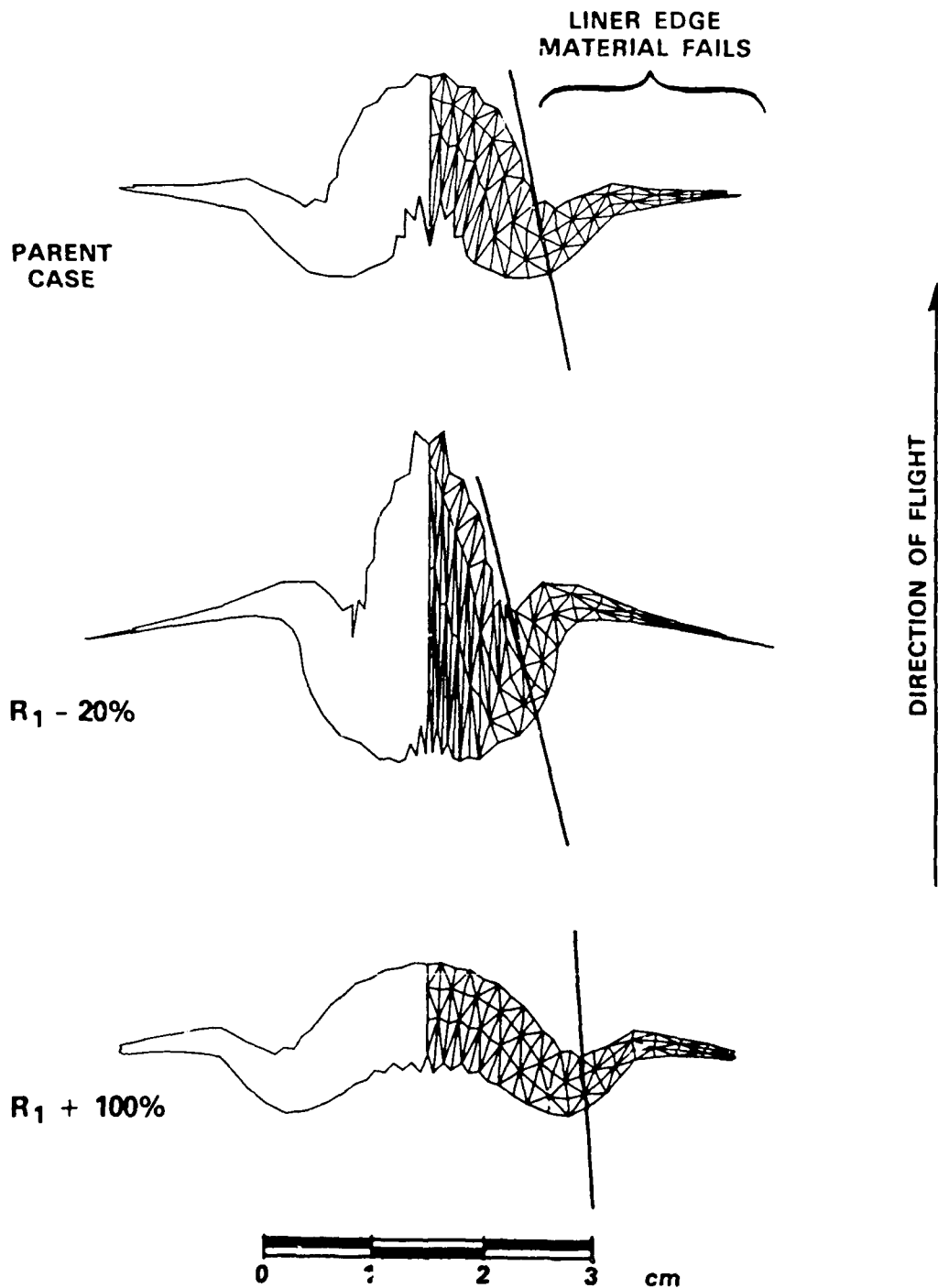


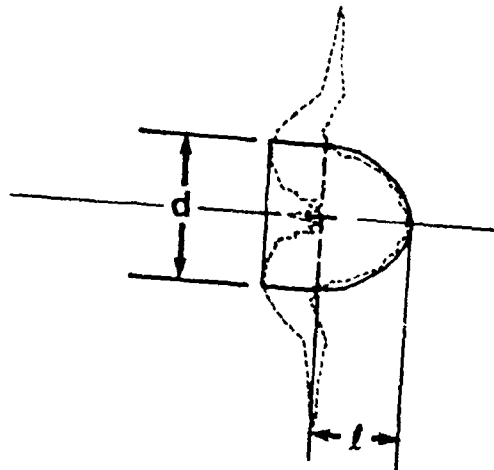
Figure 5

EXROD FINAL FRAGMENT SHAPES FOR 2 REPRESENTATIVE  
PARAMETER VARIATIONS

UNCLASSIFIED

SM 1124

EXROD



REDM

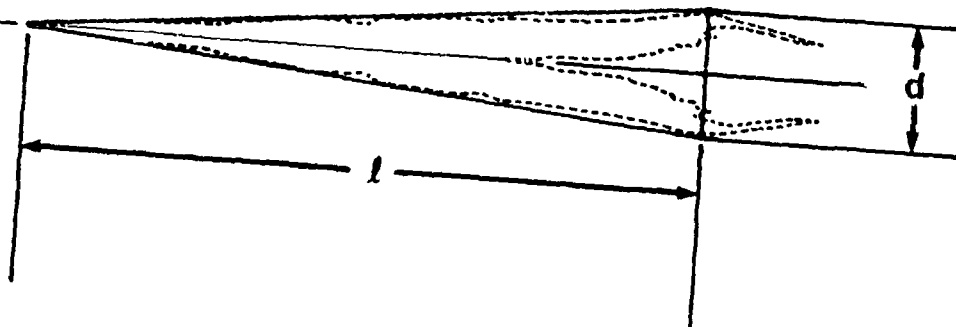


Figure 6  
DEFINITION OF THE SHAPE FACTOR  $l/d$  FOR THE  
EXROD AND REDM FRAGMENTS

UNCLASSIFIED

UNCLASSIFIED

SM 1124

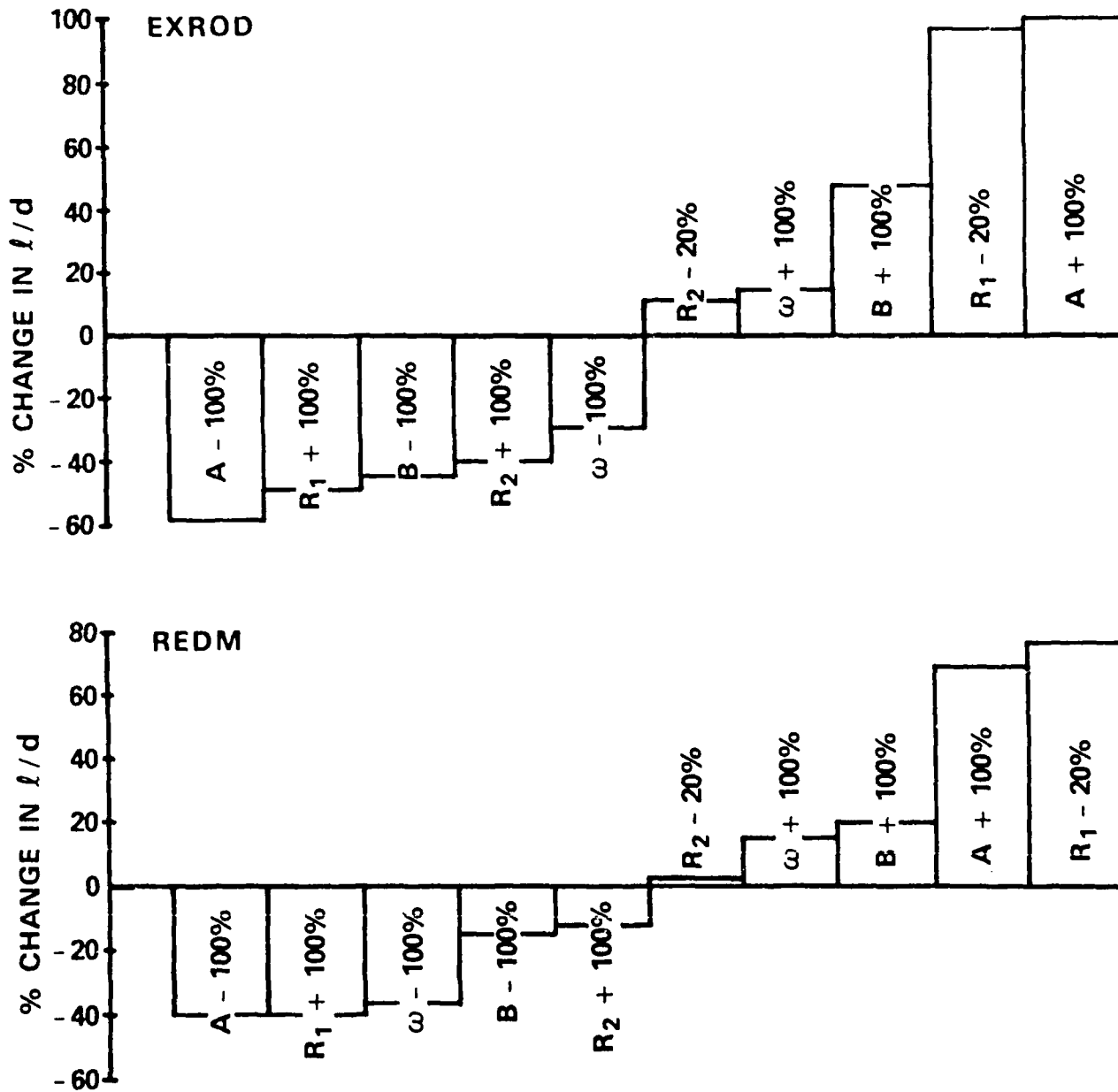


Figure 7

PERCENT CHANGES IN EXROD AND REDM SHAPE  
FACTOR ( $l/d$ ) FOR EACH PARAMETER VARIATION

UNCLASSIFIED

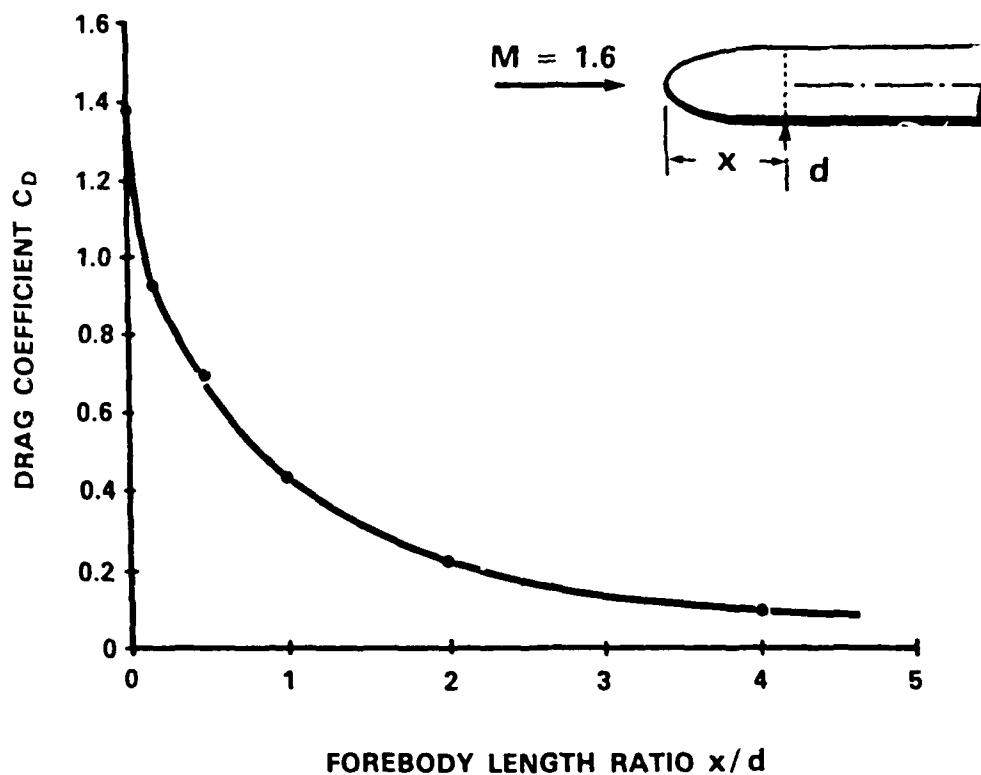


Figure 8

FOREBODY DRAG OF A GROUP OF SPHEROIDAL HEADS AS  
A FUNCTION OF FOREBODY LENGTH RATIO AT  $M = 1.6$   
(from Reference 5, Chapter 16, Figure 16)

UNCLASSIFIED

SYM 12-4

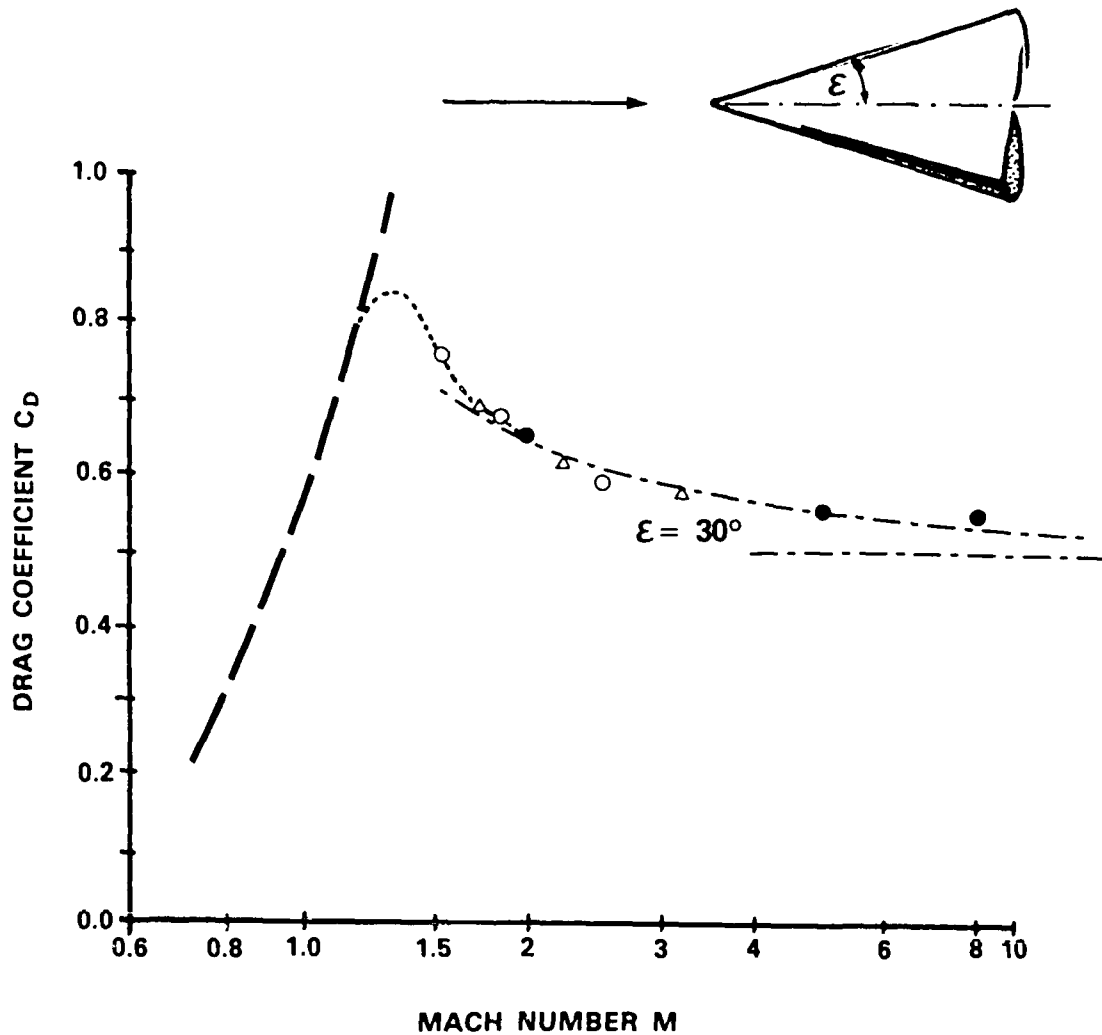


Figure 9

THEORETICAL AND EXPERIMENTAL DRAG COEFFICIENTS OF VARIOUS  
CONICAL HEADS AT TRANSONIC AND SUPERSONIC MACH NUMBERS  
(from Reference 5, Chapter 16, Figure 23)

UNCLASSIFIED

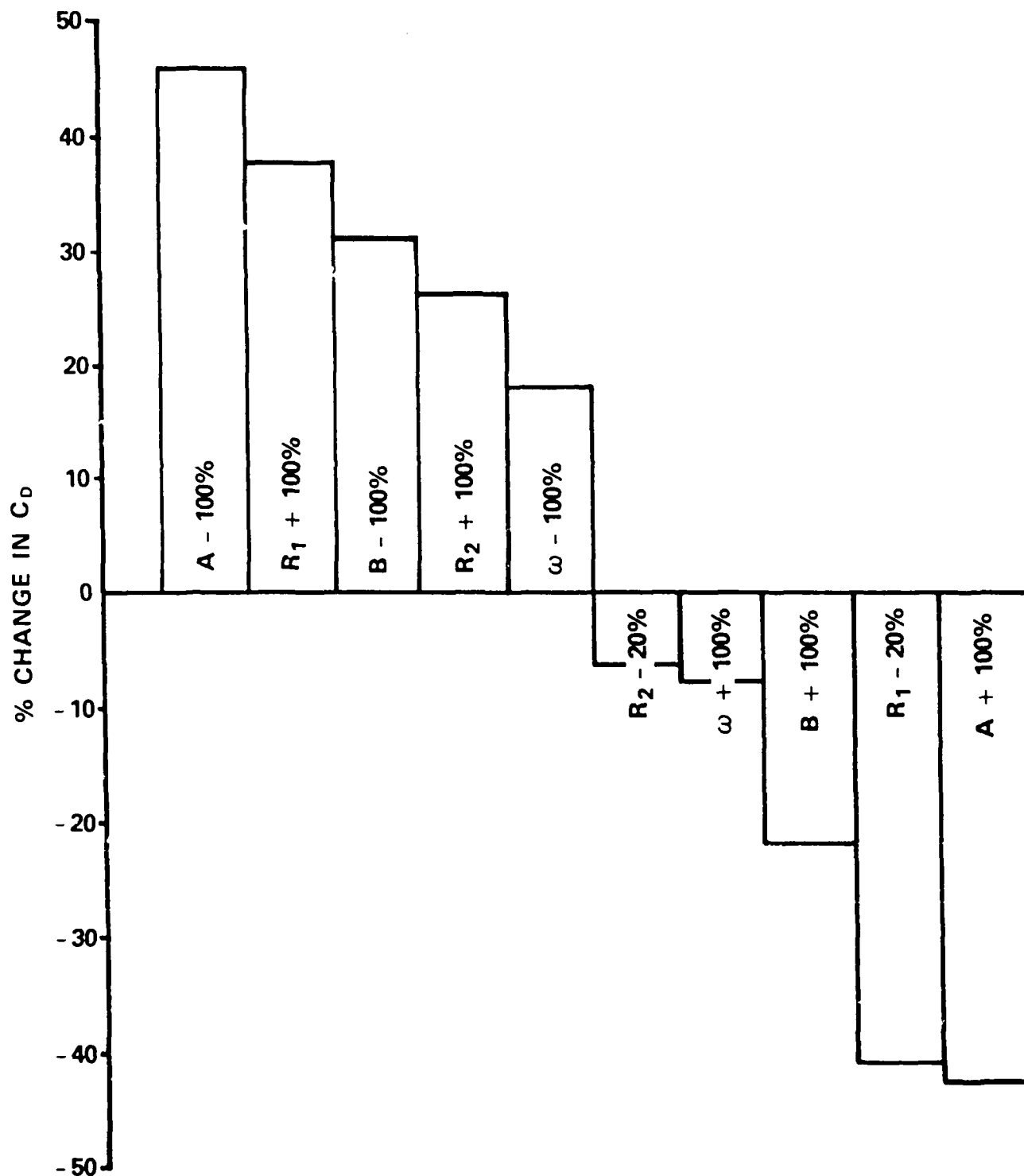


Figure 10

PERCENT CHANGES IN EXROD  $C_D$  FOR EACH  
PARAMETER VARIATION



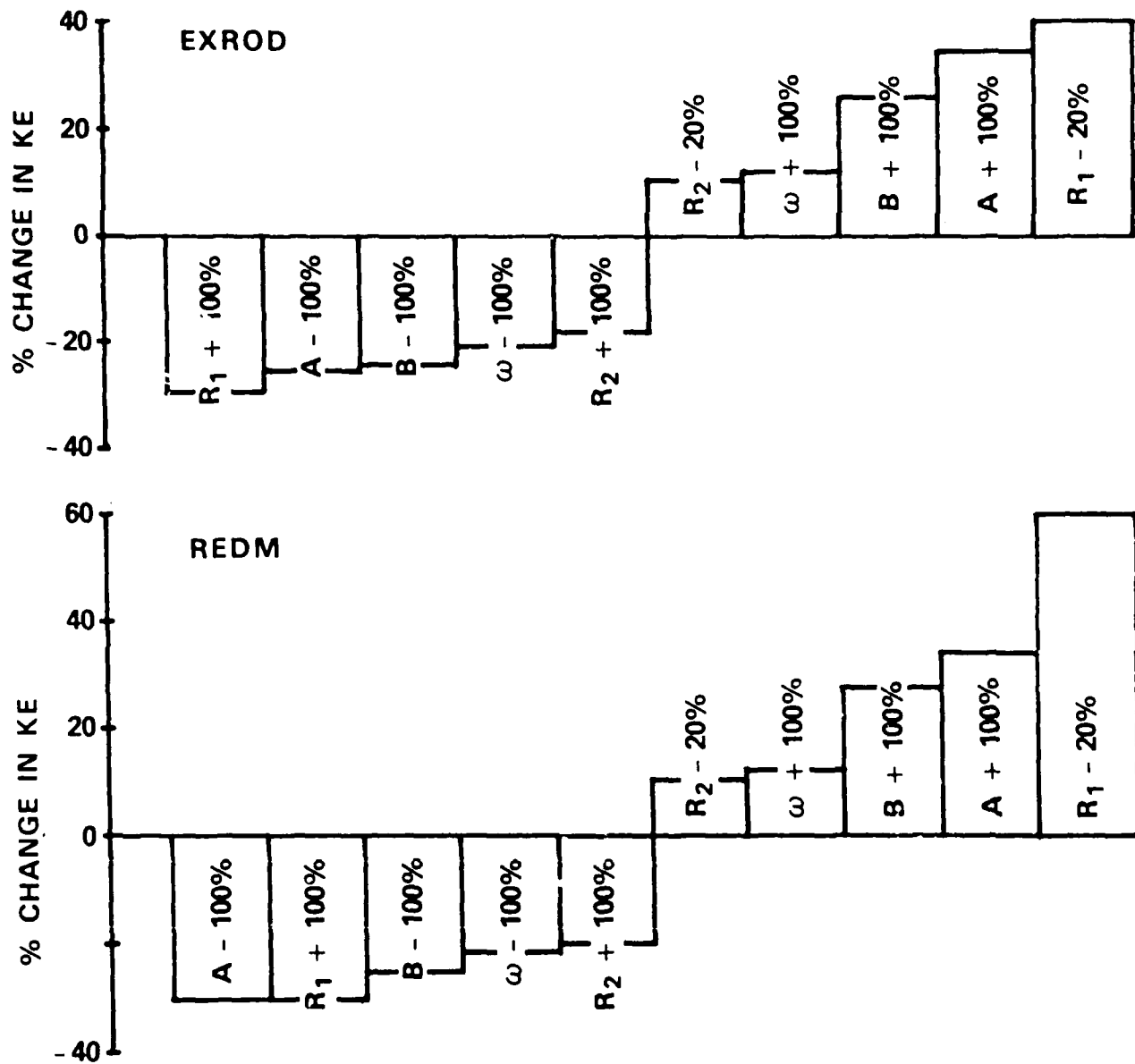


Figure 11

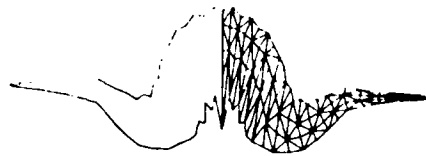
PERCENT CHANGES IN EXROD AND REDM KINETIC ENERGIES  
FOR EACH PARAMETER VARIATION

UNCLASSIFIED

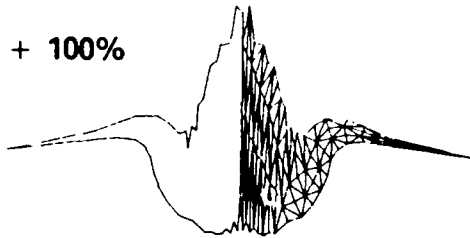
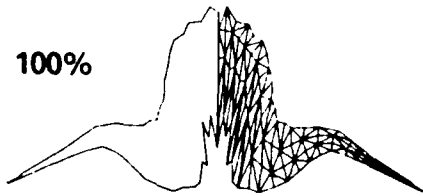
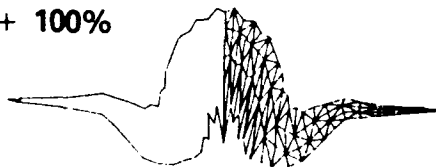
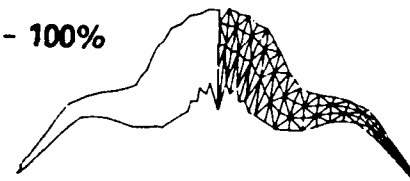
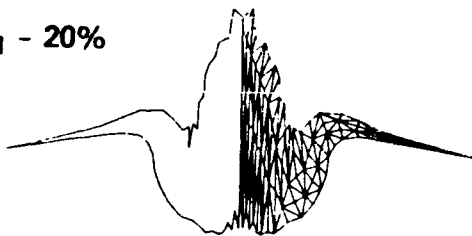
**APPENDIX**  
**EXROD AND REDM**  
**FINAL FRAGMENT SHAPES**

UNCLASSIFIED

## EXROD

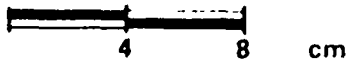


PARENT CASE

 $A + 100\%$  $A - 100\%$  $B + 100\%$  $B - 100\%$  $\omega + 100\%$  $\omega - 100\%$  $R_1 - 20\%$  $R_1 + 100\%$  $R_2 - 20\%$  $R_2 + 100\%$ 

DIRECTION OF FLIGHT

## REDM



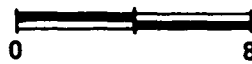
## PARENT CASE

 $A + 100\%$  $B + 100\%$  $\omega + 100\%$  $R_1 - 20\%$  $R_2 - 20\%$ 

DIRECTION OF FLIGHT

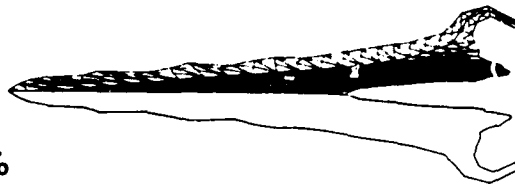


## REDM

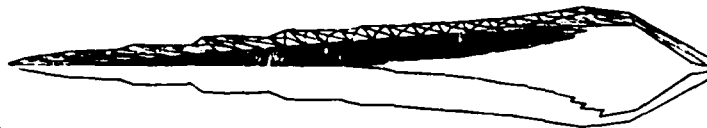
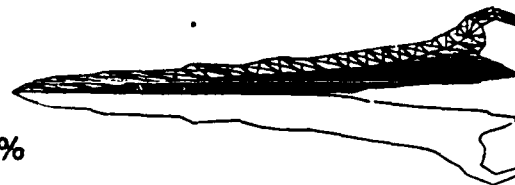


0 8 cm

A - 100%



B - 100%

 $\omega$  - 100% $R_1 + 100\%$  $R_2 + 100\%$ 

DIRECTION OF FLIGHT



**DOCUMENT CONTROL DATA - R & D**

(Security classification of title, body of abstract and indexing annotation must be entered when the overall document is classified)

1. ORIGINATING ACTIVITY  Defence Research Establishment Suffield		2a. DOCUMENT SECURITY CLASSIFICATION <b>UNCLASSIFIED</b>	
		2b. GROUP	
3. DOCUMENT TITLE Sensitivity of SFF Computer Simulations to Variations in the JWL Equation of State			
4. DESCRIPTIVE NOTES (Type of report and inclusive dates) Suffield Memorandum No. 1124			
5. AUTHOR(S) (Last name, first name, middle initial) K.R. Torrance			
6. DOCUMENT DATE January 1985		7a. TOTAL NO. OF PAGES 34	7b. NO. OF REFS 6
8a. PROJECT OR GRANT NO. 27C20		9a. ORIGINATOR'S DOCUMENT NUMBER(S) Suffield Memorandum No. 1124	
8b. CONTRACT NO.		9b. OTHER DOCUMENT NO.(S) (Any other numbers that may be assigned this document)	
10. DISTRIBUTION STATEMENT Unlimited			
11. SUPPLEMENTARY NOTES		12. SPONSORING ACTIVITY	
13. ABSTRACT  The sensitivity of predictions of self-forging fragment shape and kinetic energy to variations in the Jones-Wilkins-Lee (JWL) equation of state for the detonation products is studied parametrically using the EPIC-2 finite element computer code. JWL parameters are varied for two warhead designs: the EXROD (EXplosive Remote Opening Device) and the REDM (REsearch and Development Munition). The resulting percentage changes in shape factor and kinetic energy are presented in tabular and graphical form, and the most influential JWL parameters are identified.			

## KEY WORDS

self-forging  
fragment  
EPIC  
simulation  
JWL  
equation  
variation

## INSTRUCTIONS

1. **ORIGINATING ACTIVITY** Enter the name and address of the organization issuing the document.
- 2a. **DOCUMENT SECURITY CLASSIFICATION** Enter the overall security classification of the document including special warning terms whenever applicable.
- 2b. **GROUP** Enter security reclassification group number. The three groups are defined in Appendix "M" of the DRB Security Regulations.
3. **DOCUMENT TITLE** Enter the complete document title in all capital letters. Titles in all cases should be unclassified. If a sufficiently descriptive title cannot be selected without classification, show title classification with the usual one-capital-letter abbreviation in parentheses immediately following the title.
4. **DESCRIPTIVE NOTES** Enter the category of document, e.g. technical report, technical note or technical letter. If appropriate, enter the type of document, e.g. interim, progress, summary, annual or final. Give the inclusive dates when a specific reporting period is covered.
5. **AUTHOR(S)** Enter the name(s) of author(s) as shown on or in the document. Enter last name, first name, middle initial. If military, show rank. The name of the principal author is an absolute minimum requirement.
6. **DOCUMENT DATE** Enter the date (month, year) of Establishment approval for publication of the document.
- 7a. **TOTAL NUMBER OF PAGES** The total page count should follow normal pagination procedures, i.e., enter the number of pages containing information.
- 7b. **NUMBER OF REFERENCES** Enter the total number of references cited in the document.
- 8a. **PROJECT OR GRANT NUMBER** If appropriate, enter the applicable research and development project or grant number under which the document was written.
- 8b. **CONTRACT NUMBER** If appropriate, enter the applicable number under which the document was written.
- 9a. **ORIGINATOR'S DOCUMENT NUMBER(S)** Enter the official document number by which the document will be identified and controlled by the originating activity. This number must be unique to this document.
- 9b. **OTHER DOCUMENT NUMBER(S)** If the document has been assigned any other document numbers (either by the originator or by the sponsor), also enter this number(s).
10. **DISTRIBUTION STATEMENT** Enter any limitations on further dissemination of the document, other than those imposed by security classification, using standard statements such as:
  - (1) "Qualified requesters may obtain copies of this document from their defence documentation center."
  - (2) "Announcement and dissemination of this document is not authorized without prior approval from originating activity."
11. **SUPPLEMENTARY NOTES** Use for additional explanatory notes.
12. **SPONSORING ACTIVITY** Enter the name of the departmental project office or laboratory sponsoring the research and development. Include address.
13. **ABSTRACT** Enter an abstract giving a brief and factual summary of the document, even though it may also appear elsewhere in the body of the document itself. It is highly desirable that the abstract of classified documents be unclassified. Each paragraph of the abstract shall end with an indication of the security classification of the information in the paragraph (unless the document itself is unclassified) represented as (TS), (S), (C), (R), or (U).  
  
The length of the abstract should be limited to 20 single-spaced standard typewritten lines; 7 1/4 inches long.
14. **KEY WORDS** Key words are technically meaningful terms or short phrases that characterize a document and could be helpful in cataloging the document. Key words should be selected so that no security classification is required. Identifiers, such as equipment model designation, trade name, military project code name, geographic location, may be used as key words but will be followed by an indication of technical context.

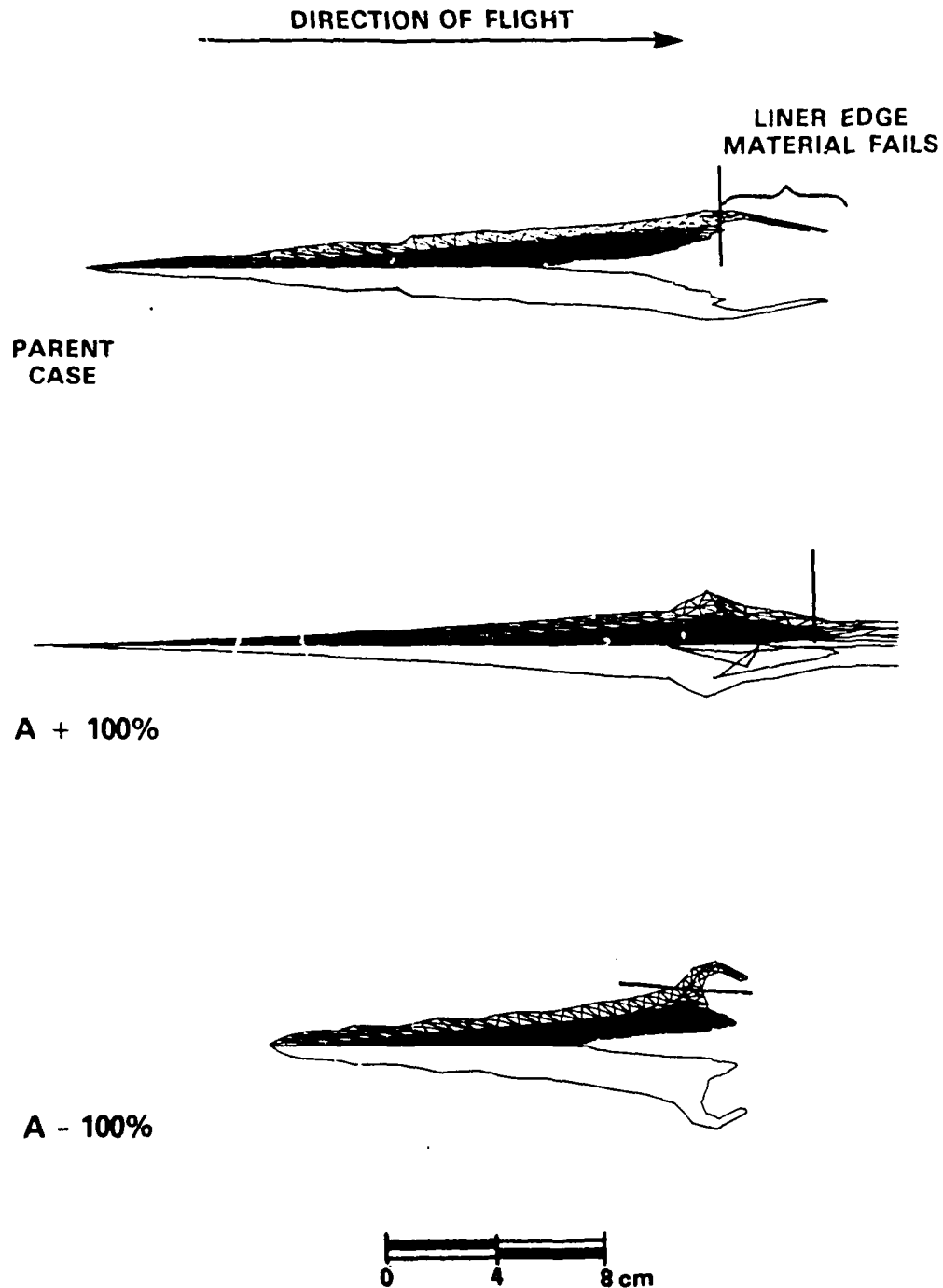


Figure 4

REDM FINAL FRAGMENT SHAPES FOR 2 REPRESENTATIVE  
PARAMETER VARIATIONS